International Journal of Environmental Science and Technology (2025) 22:13927–13946
https://doi.org/10.1007/s13762-025-06527-w

ORIGINAL PAPER

Analysis of vegetation response to four climate factors based on the CTSS-RESTREND method

B. Hao[1] · S. Ding[1] · Z. Wu[1] · Z. Ruan[2] · L. Mai[1] · Y. Kuang[1]

Received: 15 January 2025 / Revised: 4 March 2025 / Accepted: 15 April 2025 / Published online: 21 May 2025
© The Author(s) 2025

Abstract

Climate change significantly influences vegetation growth, necessitating an in-depth understanding of the climate-driven dynamics of vegetation to formulate ecological and environmental policies. This study addresses the limitations of traditional correlation analysis methods by utilizing a combined approach of Residual Trend Analysis (RESTREND) and Time Series Segmentation Residual Trend Analysis (TSS-RESTREND), known as CTSS-RESTREND. By using this method, we examined the influence of near-surface air temperature, precipitation, humidity, and wind speed on vegetation growth in Guangdong Province from 2000 to 2020, using Normalized Difference Vegetation Index (NDVI) data and climatic variables. Using MOD13Q1 NDVI data and ERA5 downscaled climate reanalysis data, this research utilizes the CTSS-RESTREND algorithm to quantify the climate effects on vegetation. The analysis reveals that precipitation and humidity are the primary positive drivers of vegetation growth, temperature has a slightly higher positive than negative impact on vegetation, while wind speed generally has a negative impact on vegetation, but its effect is relatively slight. During the growing season, the growth of vegetation becomes more sensitive to the three climatic factors: temperature, precipitation, and humidity. This study provides a more accurate and detailed understanding of the spatiotemporal changes and climate driving factors affecting vegetation in Guangdong Province.

Keywords Guangdong Province · NDVI · CTSS-RESTREND · Climate change · Vegetation growth

Introduction

Vegetation, as a vital component of terrestrial ecosystems, plays a pivotal role in the Earth's carbon cycle and significantly influences ecosystem stability (Yang and Guan 2006; Zhao et al. 2022; Chu et al. 2019). Monitoring and analyzing vegetation changes is essential for assessing changes in regional and global ecological environments (Ivits et al 2014; Liu et al. 2017; Martinez and Labib 2023). The Normalized Difference Vegetation Index (NDVI) serves as an indicator of vegetation productivity and is widely used to monitor dynamic changes in vegetation growth (Londhe et al. 2024; Tang et al. 2015; Wen et al. 2017; Zhang Y and Ye 2020). Analyzing spatiotemporal variations in NDVI provides valuable insights into regional vegetation dynamics (Sun et al. 2015). By combining this analysis with driving factor analysis, we can effectively evaluate the impact of climate change and human activities on vegetation dynamics (Ma et al. 2017; Sun et al. 2023; Li et al. 2013). However, due to regional disparities, diverse vegetation types, and variations in climate conditions, multiple driving factors have complex and variable impacts on vegetation (L F Zhang et al 2022a, b; Yan et al. 2023; Gong et al. 2022; Zhong et al. 2010). For instance, the influence of wind speed on vegetation growth varies significantly across regions and vegetation types (T. Zhang et al. 2022a, b). Therefore, conducting quantitative research on the impact of various driving factors on vegetation growth holds great significance.

Climate change have a significant impact on vegetation growth (Piao et al. 2020; Wang et al. 2015; Mohammat et al. 2013; De Jong et al. 2013). Changes in climate conditions can affect the air and soil environments, consequently altering the nutrient transport of vegetation and

Editorial responsibility: Samareh Mirkia.

✉ Y. Kuang
kuangyaoqiu@jnu.edu.cn

[1] College of Environment and Climate, Jinan University, Guangzhou 511443, China

[2] School of Geography and Tourism, Huizhou University, Huizhou 516007, China

disrupting its original growth patterns (Tietjen et al. 2017; Sun et al. 2022). As a result, the influence of climate change on vegetation exhibits a time lag and is influenced by various vegetation types and regional disparities (Kong et al. 2020). Moreover, the process of climate-induced vegetation change is inherently complex. In addition to regional variations, the impact of a particular climate factor on vegetation is influenced by natural factors such as slope direction and elevation, leading to a complex driving mechanism (Zhang et al. 2024; Boulion 2017). To investigate the relationships between climate factors and vegetation change, Guo et al. analyzed the global NDVI change trend from 1982 to 2014 and the driving effect of climate on NDVI. The results showed that NDVI showed a significant upward trend from 1982 to 2014, and the increase in the Northern Hemisphere was higher than that in the Southern Hemisphere (Guo et al. 2022). Among various climate factors, temperature and precipitation have a significant impact on NDVI (Chuai et al. 2013; Cao et al. 2011; Morovati and Karami 2024; Hilker et al. 2014). It is worth mentioning that the effects of temperature and precipitation on NDVI differ due to variations in geographical and climatic conditions between the two hemispheres. In the Northern Hemisphere, temperature plays a predominant role as a climate driver for NDVI, while precipitation takes on this role in the Southern Hemisphere (Hou etn al. 2013). In equatorial regions, temperature primarily controls NDVI changes, particularly during the spring and autumn seasons. Notably, the impact of climate on vegetation is more pronounced in arid areas (Ichii et al. 2002). Han et al. demonstrated that climate change plays a pivotal role in driving vegetation changes in arid regions (Han et al. 2021). Due to the continuous enhancement of climate change, the impact of climate on vegetation and ecological environment has become increasingly evident. In order to analyze the impact of climate change on vegetation, Abeli et al. analyzed the impact of European summer heatwaves on wildlife. The results demonstrated that wildlife is highly vulnerable to the negative impacts of extreme weather events and their direct and indirect consequences. European heatwaves can cause a decrease in precipitation, which affects plant physiology and metabolism, thereby affecting plant growth and reproduction. The main consequence is vegetation adaptation or extinction (Abeli et al. 2014). Climate-driven vegetation displays spatial heterogeneity, resulting in significant variations in the time lag of vegetation response (Wu et al. 2015; Duan et al. 2021; Sedighifar et al. 2020). In order to study the hysteresis of climate driven vegetation change, Wu et al. used the GIMMS3g NDVI time series and CRU temperature, precipitation, and solar radiation datasets to quantitatively determine the time delay effects of global vegetation response on different climate factors. The results indicate that there are significant global differences in the time lag effect of vegetation response and the main climate driving factors that significantly affect vegetation growth, which is related to the diversity of vegetation and climate characteristics (Wu et al. 2015). In order to study the driving effect of more climate factors on vegetation change, Mao et al. studied the impact of climate factors such as temperature, precipitation, sunshine, potential evaporation, and water vapor pressure on vegetation in northern Tibet, China. The results show that the most important climate factor affecting NDVI annual change is temperature (Mao et al. 2007).

At present, the research methods on vegetation change driven by climate factors in China are mainly based on correlation analysis, and the results are relatively rough (Song and Ma, 2017; Guan et al. 2020; He et al. 2018; Gao et al. 2021; Xu et al. 2019). To solve this problem, this study selects Guangdong Province as the study area. Guangdong Province is located in the southernmost part of Chinese Mainland, adjacent to the South China Sea, and is more vulnerable to extreme climate events such as typhoons. Climate change has a greater impact on the ecological environment, which is of high research significance. The combined algorithm CTSS-RESTREND (Combine RESTREND and TSS-RESTREND) (Ruan et al. 2020) based on RESTREND (residual trend analysis) (Li et al. 2016; Chen et al. 2018) and TSS-RESTREND (Liu et al. 2019) (Time Series Segmentation Residual Trend Analysis) is applied to analyze the vegetation response to climate change in Guangdong Province from 2000 to 2020. The results presented in the form of slope are more accurate than the correlation analysis, and the combination can effectively solve the problem of the defect as insufficient number of significant pixels caused by multi-step tests of RESTREND and TSS-RESTREND, and obtain fine results of climate-driven vegetation effects.

Materials and methods

Study area

Guangdong Province is located in the south of the Nanling Mountain, bordering Hong Kong, Macao, Guangxi, Hunan, Jiangxi and Fujian, with Nanling Mountain in the north, Mount Wuyi in the northeast, South China Sea in the south and Taiwan across the strait in the east, with a geographical coordinate of 109°39′-117°19′E and 20°13′-25°31′N (Fig. 1). The land area of Guangdong Province is $17.98 \times 104 km^2$, with a coastline of 3368.1 km. As it is close to the sea and has a long coastline, it is vulnerable to typhoons from the Western Pacific and South China Sea. Windstorms, heavy rains and flood disasters caused by typhoons are quite serious (Li et al. 2021; Zhang et al. 2011). In consideration of the climatic characteristics of Guangdong Province, four climatic factors: temperature,

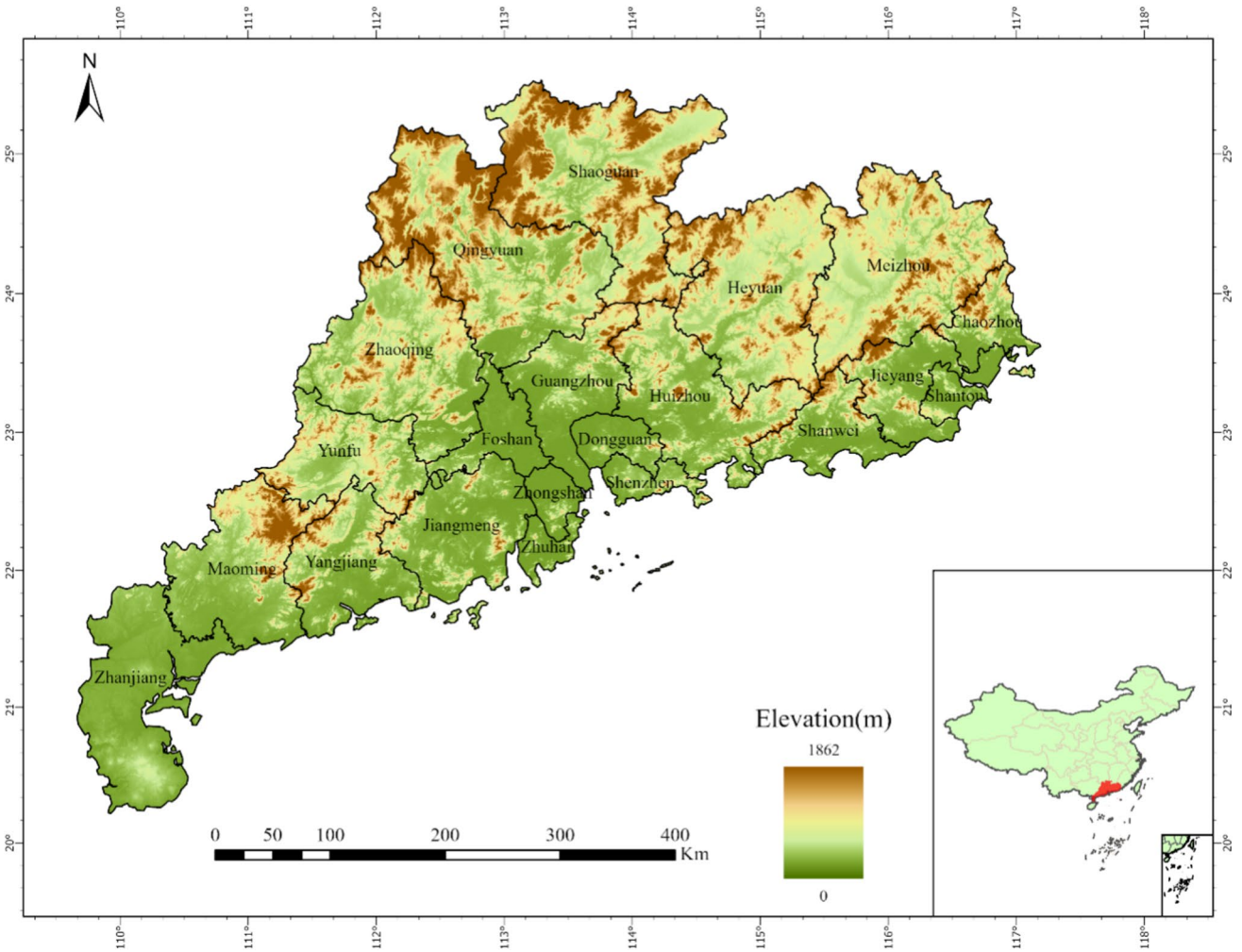


Fig. 1 Location of the Guangdong Province

precipitation, humidity, and wind speed were selected to analyze the vegetation's responses to these factors.

Data collection

The NDVI data used in this paper is downloaded from the MOD13Q1 product by Google Earth Engine, with a time resolution of 16d, a spatial resolution of 250 m, and a time range from 2000 to 2020. To ensure the accuracy of pixel-level trend analysis, the Savitzky-Golay (S-G) filter was employed to assign weight coefficients based on quality assessment (QA) values from the MOD13Q1 NDVI data. This approach effectively eliminates effects from noises, such as those caused by clouds and rain, thereby producing high-quality NDVI time series data for reliable trend detection. (Huang et al. 2018; Meng et al. 2017). The specific assignment values are as follows:

The higher the QA value, the greater the noise in the image, and a lower weight should be assigned; The lower the QA value, the smaller the image noise, and a higher weight should be assigned. Therefore, assigning a weight of 1 to a low noise pixel with a QA value of 0; assign a weight of 0.5 to pixels with a QA value of 1; High noise pixels with QA values of 2–3 are assigned a weight of 0.2 and reconstructed using S-G filter. Synthesize the maximum value of filtered MODIS NDVI data into monthly NDVI data to further remove noise effects such as clouds and rain. Utilizing the cropping tools and grid to projection tools in ArcMap, the study area was cropped and transformed into a high-quality monthly NDVI TIFF dataset for Guangdong Province from 2000 to 2020.

Four climate factor data downloaded from ERA5 downscaling reanalysis climate data set of National Earth System Science Data Center(http://www.geodata.cn), mainly includes temperature (in this study, the temperature data is near surface temperature data, and the temperatures

mentioned later represent near surface temperature), precipitation, humidity (relative humidity data), and wind speed for reanalysis of four climate factor data. The time resolution is one month, the spatial resolution is 1 km, and the time range is from 2000 to 2020. Using Python to convert it to points and using inverse distance weight interpolation in ArcGIS, the climate factor data is interpolated to a spatial resolution of 250 m, and then cropped and projected to obtain climate factor data corresponding to NDVI data.

Methods

Using the processed NDVI data, the NDVI values at inter-annual, growing season, and seasonal scales were calculated. Break-point analysis was conducted to examine the variation trends, abrupt changes, and distribution characteristics of NDVI in Guangdong Province. Processed climate variable data were also analyzed at inter-annual and seasonal scales to detect the variation trends and spatial characteristics of the four climate factors in Guangdong Province. Vegetation response to climate factors exhibits a certain lag, generally not exceeding one month (Kuzya-kov and Gavrichkova, 2010; Chapin and Starfield 1997; Davis 1989). Consequently, the NDVI data were shifted by one month to correspond with the four climate factor datasets. RESTREND (residual trend) and TSS-RESTREND (time-series segmentation and residual trend) analyses were employed to isolate the combined effects of climate factors, with the results subsequently merged to form CTSS-RESTREND (combining time-series segmentation and residual trend with residual trend). This methodology increases the number of valid pixels, enabling the analysis of vegetation responses to individual climate factor in Guangdong Province (Fig. 2).

Univariate linear regression

In time series analysis, the univariate linear regression method is commonly employed. This method is used to calculate the temporal trends of climatic factors and vegetation indices within the study area. By conducting a pixel-by-pixel analysis of the slope of changes over the study period, the spatial distribution of the overall trends for both climatic factors and vegetation indices can be determined. Here, x_i represents the vegetation indices and climatic factors, and t_i represents time. A univariate linear regression equation is constructed for x_i and t_i, as shown in Eq. (1).

$$x_i = at_i + b, (i = 1, 2, 3...n) \tag{1}$$

In the linear regression analysis of climate factors, a represents the regression coefficient, and b denotes the constant term. Due to the generally low overall trend changes, which fail to adequately capture variation differences, the slope of the climate factor regression is expressed as ten times the regression coefficient to enhance visibility of the changes (Hou et al. 2013).

Mann–Kendall mutation test

The Mann–Kendall mutation test, as a commonly used non-parametric method, is widely applied in long-term time series studies because its results are not influenced by individual outliers. The test statistic, denoted as the Z value, is typically represented by the following formula.

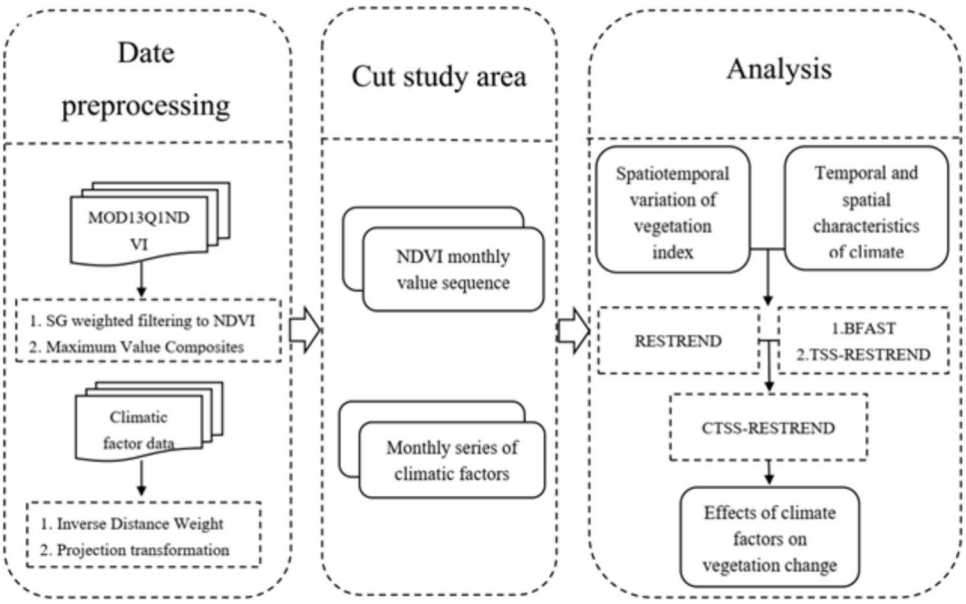


Fig. 2 The flowchart of methods

$$Z = \begin{cases} \frac{S}{\sqrt{var}}(S > 0) \\ 0(S = 0) \\ \frac{S+1}{\sqrt{var}}(S < 0) \end{cases} \quad (2)$$

$$S = \sum_{i=1}^{n-1} \sum_{j=i+1}^{n} \text{sign}(x_j - x_i) \quad (3)$$

$$\text{sign}(\theta) = \begin{cases} 1(x_j - x_i) > 0 \\ 0(x_j - x_i) = 0 \\ -1(x_j - x_i) < 0 \end{cases} \quad (4)$$

$$\text{Var}(S_k) = \frac{n(n-1)(2n+5)}{18} \quad (5)$$

In Eqs. (3)-(5), n represents the total number of observations, and x_j and x_i denote the time series data. When the test statistic Z in Eq. (2) is greater than 1.96, the trend changing results pass the significance test at a 95% confidence level, indicating a significant change. Otherwise, the change is not considered significant.

Coefficient of variation

The coefficient of variation can reflect the stability of spatial variation in vegetation through the ratio of the standard deviation to the mean. The specific calculation formula is as follows:

$$CV = \frac{SD_{NDVI}}{M_{NDVI}} \quad (6)$$

In Eq. (6), SD_{NDVI} represents the standard deviation of the annual mean NDVI in Guangdong Province, while M_{NDVI} denotes the average NDVI value for each year in Guangdong Province. Based on the calculated CV values, the stability of vegetation in the study area is classified into three levels: stable regions ($CV \leq 15\%$), unstable regions ($15\% < CV \leq 40\%$), and highly unstable regions ($CV > 40\%$).

BFAST

The BFAST (Breaks for Additive Seasonal and Trend) algorithm is an iterative linear fitting season and trend model proposed by Verbeselt et al. in 2010 (Verbesselt et al. 2010). It divides the time series into seasonal components, trend components, and residual components, and can detect time series mutation points in trend components. The general expression of the model is shown in Eq. (7):

$$Y_t = T_t + S_t + e_t, (t = 1,\ldots, n) \quad (7)$$

In the equation, Y_t represents the observed values of the time series, and in this study, it represents the NDVI value; T_t represents the trend component; S_t represents the seasonal component; e_t represents the residual component; t represents time. When set as linear during fitting, with mutation points of $t_1^*,\ldots,t_m^*$, it can be represented by Eq. (8):

$$T_t = \alpha_j + \beta_j t, \quad (8)$$

α_j represents the intercept; β_j represents the slope; j represents the time between two mutation points. The amplitude and direction of the mutation point are determined by the sum on both sides of the break-points.

The seasonal components S_t are fitted using a segmented seasonal model, and the specific calculation formula is as follows:

$$S_t = \sum_{k=1}^{i} \alpha_{i,k} sin\left(\frac{2\pi kt}{f} + \delta_{i,k}\right), \quad (9)$$

i represents the break-point position; k represents the number of harmonic terms in the periodic model; $\delta_{i,k}$ represents the time item; f represents frequency. BFAST will input the calculation results back into the iteration when calculating the break-point, hence high calculation accuracy can be obtained.

In the study of NDVI time series, the BFAST algorithm can eliminate the NDVI changes caused by seasonal vegetation growth, and detect the location of break-points and sudden variables through linear fitting using the least square method. Due to the removal of seasonal NDVI changes before calculating the break-points, that detected in the trend component, are mainly caused by extreme climate change and human activities.

In this study, the BFAST algorithm was implemented using the "bfast" toolkit in version 4.0.3 of the R language.

RESTREND

RESTREND is a commonly used method for detecting vegetation changes (Ibrahim et al. 2015; Kundu et al. 2017). It separates the effects of various driving factors by calculating residuals and performs linear regression, with the formula as follows:

$$y = a_1x_1 + a_2x_2 + a_3x_3 + a_4x_4 + b_1, \quad (10)$$

$$\varepsilon = y' - y, \quad (11)$$

y represents the NDVI values affected by four climate factors, x_1, x_2, x_3 and x_4 represent the four climate factors in this study a_1, a_2, a_3 and a_4 represent regression coefficients; b_1 represents intercept; y' represents the NDVI value; ε represents residual.

Perform stepwise residual calculation using the RESTREND algorithm, the response results of vegetation to individual climate factors can be separated (First, calculate the NDVI values affected by four climate factors, and then perform residuals. At this time, the residuals represent the NDVI changes affected by other factors except for the four climate factors. Then, calculate the NDVI values affected by three of the climate factors. At this time, the residuals represent the remaining NDVI changes affected by one climate factor and other factors. By subtracting the residuals from the two, the impact of a single climate factor on NDVI can be disintegrated.) By performing a univariate linear fitting of the residual amount to calculate its trend change, the rate of vegetation change can be obtained, which is more intuitive in the results.

In this study, the RESTREND algorithm was implemented in version 4.0.3 of the R language.

TSS-RESTREND

TSS RESTREND is an extended algorithm in residual trend analysis, which combines break-points with linear regression to detect the driving effects of climate factors on vegetation in segments (Burrell et al. 2017). The formula is as follows:

$$y_s = a_1x_1 + a_2x_2 + a_3x_3 + a_4x_4 + a_5z + a_6x_1z + a_7x_2z + a_8x_3z + a_9x_4z + b_2, \quad (12)$$

Formula (12) is a piecewise linear regression equation used to fit the relationship between vegetation and climate factors, where y_s represents the NDVI value, x_1, x_2, x_3 and x_4 respectively represent four climate factors, a_1~a_9 is the regression coefficient, b_2 is the intercept, and z is the dummy variable (0 or 1). In this study, the dummy variable is represented by the break-point of BFAST. The value of linear fitting before the break-point is 0, and the value after the break-point is 1. Its significance is calculated by the Chow test.

$$\varepsilon_s = y_s - y'_s, \quad (13)$$

ε_s represents residual, and the results of the impact of different types of climate factors on vegetation using Eq. (12) are continuously calculated using Eq. (13) to obtain the impact of a single climate factor on vegetation. The results are fitted linearly to obtain the change rate of the impact of a single climate factor on vegetation.

In this study, the TSS-RESTREND algorithm was implemented in version 4.0.3 of the R language.

CTSS-RESTREND

Although the RESTREND and TSS-RESTREND algorithms can strip out the influence of individual driving factors, the two-step test (residual and linear fitting) greatly reduces the number of significant pixels, which is not conducive to analysis. In order to solve this problem, Ruan et al. proposed the CTSS-RESTREND (Combine TSS-RESTREND with RESTREND) algorithm in 2020 (Ruan et al. 2020). CTSS-RESTREND can add up the number of significant pixels calculated by RESTREND and TSS-RESTREND algorithms, greatly increasing the number of significant pixels. Specifically, in the CTSS-RESTREND algorithm, the integration of TSS-RESTREND and RESTREND is efficiently achieved through the raster calculator in ArcGIS. This process utilizes the mathematical logic function (IsNull) and the conditional function (con) in the raster calculator. First, the IsNull function is used to identify pixels with insignificant changes in the TSS-RESTREND analysis; then, the con function selects pixels with significant changes in the RESTREND analysis. The combined result can increase the number of significant pixels, thereby enabling a more precise analysis of vegetation climate driving factors. The expression for this process is given in Eq. (14), and the specific operation workflow is shown in Fig. 3.

$$\text{Result} = \text{con}\left(\text{IsNull}\left(\text{Raster}_1\right), \text{Raster}_2, \text{Raster}_1\right), \quad (14)$$

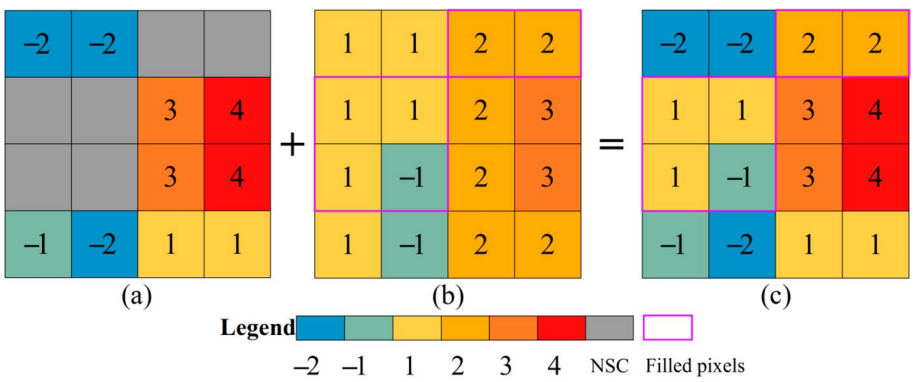


Fig. 3 The implementation of CTSS-RESSTREND in ArcGIS (Ruan et al. 2020) (a) pixels identified using TSS-RESSTREND, (b) pixels identified using RESTREND, and (c) the composite result derived from CTSS-RESSTREND. RESTREND's significant pixels fill TSS-RESTREND gaps from NSC (no significant change) pixels

Where Result represents the calculation results of CTSS-RESTREND, $Raster_1$ represents the grid layer of RESTREND calculation results, and $Raster_2$ represents the grid layer of TSS-RESTREND calculation results.

Results and discussion

Spatiotemporal variations of NDVI and climate factors

The 21-year average NDVI for Guangdong Province from 2000 to 2020 was calculated using Univariate Linear Regression, and the results are shown in Fig. 4a. The data indicated that the 21-year average NDVI values across pixels in Guangdong Province range from -0.01 to 0.90, with an overall regional average of 0.60, indicating a generally high vegetation coverage. However, some areas exhibit lower values. Regions with lower vegetation coverage (NDVI < 0.40) were mainly concentrated in the central Pearl River Delta, where urbanization is high, accounting for approximately 14.32% of the pixels. Another portion with slightly lower vegetation coverage (0.40 < NDVI < 0.60) was mainly distributed in the southwestern cities of Zhanjiang and Maoming, representing about 21.76% of the pixels. The remaining areas of the study region generally had high vegetation coverage, with NDVI values between 0.60 and 0.90 accounting for as much as 57.86% of the pixels. Overall, vegetation growth conditions in Guangdong Province were favorable, with high vegetation coverage. The trend of NDVI changes in the study region from 2000 to 2020 is shown in Fig. 4b. Using univariate linear regression, the data revealed that NDVI in the study area has generally increased over the past 21 years. Since the annual change rate of NDVI is relatively small, directly using annual data is not intuitive. Therefore, we calculated the change rate over a ten-year scale and obtained an overall change rate of 0.039 $(10a)^{-1}$, indicating a positive trend in vegetation growth.

The spatial change rate of NDVI in the study area from 2000 to 2020 was calculated using univariate linear regression, which determined the annual change rate for each pixel. The results were then subjected to the Mann–Kendall (MK) test to assess the statistical significance of these trends, as illustrated in Fig. 4c. In the MK test, change rates that pass the significance level of $p = 0.05$ are considered significant, while those that do not pass are considered non-significant. In this study, since the number of non-significant pixels was relatively small, they were classified into the category of change rate equal to 0. As shown in Fig. 4c, the change rate of NDVI in the study area from 2000 to 2020 mainly ranges between -0.36 and 0.35 $(10a)^{-1}$. The majority of pixels showed a significant upward trend,

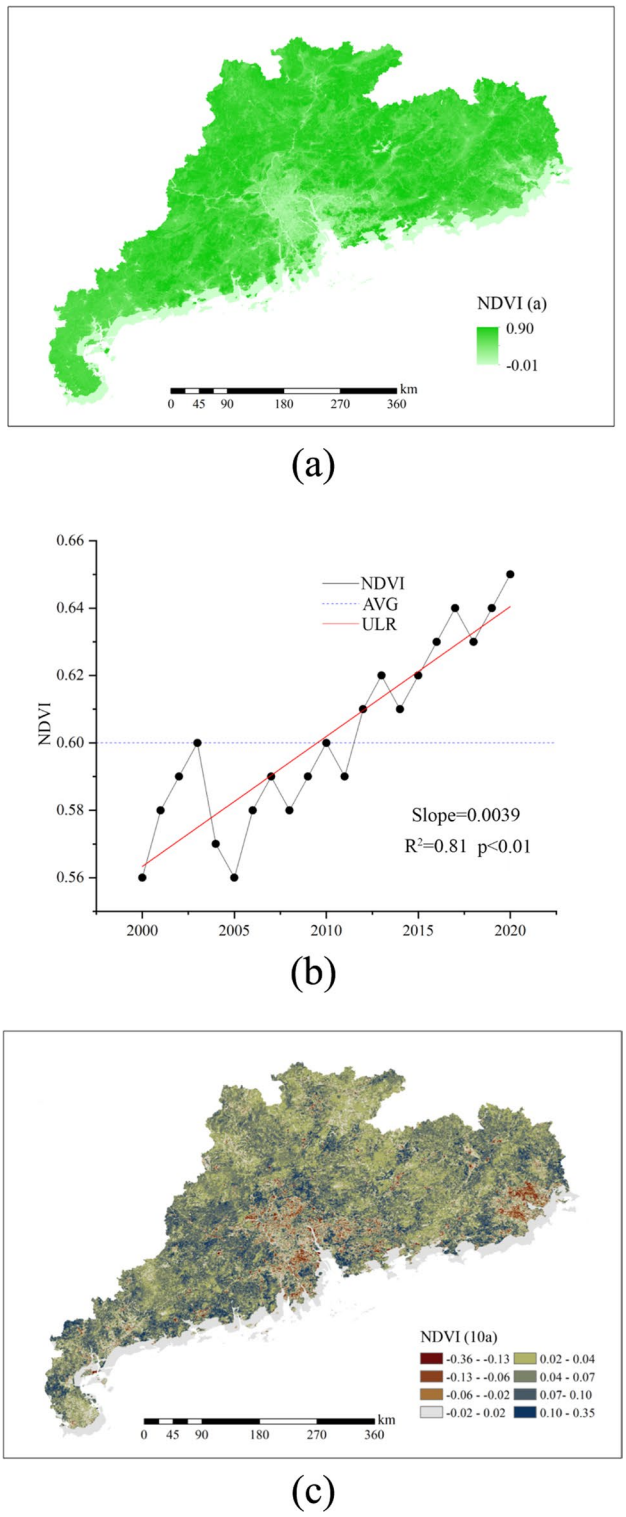


Fig. 4 Average NDVI in Guangdong Province from 2000 to 2020(a). Trend of annual NDVI in Guangdong Province from 2000 to 2020(b). The spatial distribution of the NDVI change rate in Guangdong Province from 2000 to 2020(c)

accounting for 78.86% of the pixels. Among the pixels with a significant upward trend, most had change rates between 0.02 and 0.07 $(10a)^{-1}$, indicating a slight upward trend and accounting for 49.25% of the pixels. Pixels with a larger upward trend were mainly distributed in the southern part of the study area, with change rates between 0.07 and 0.35 $(10a)^{-1}$, accounting for 18.74% of the pixels. Pixels showing a significant downward trend were primarily located in the central Pearl River Delta and the eastern part of the study area, with NDVI change rates mainly ranging from -0.36 to -0.06 $(10a)^{-1}$, accounting for 16.13% of the pixels, with a large proportion of pixels having change rates between -0.36 and -0.13 $(10a)^{-1}$, accounting for 9.86%. Overall, vegetation growth in the study area remains stable, with regions showing positive growth generally having lower vegetation change rates. In contrast, regions with negative growth rates tended to have higher rates of change, concentrated mainly in economically developed areas such as the Pearl River Delta and the Hanjiang-Rongjiang Delta.

The spatial distribution characteristics of climate elements in the study area from 2000 to 2020 are as follows: The average temperature ranged from 5 to 30℃, predominantly between 20 and 30℃. The Pearl River Delta region exhibited higher temperatures (25–30℃), while the northern region had lower temperatures (5–15℃) (Fig. 5a). The annual average precipitation ranged from 883.5 to 3169.7 mm, with most areas receiving between 1700 and 3000 mm of rainfall. Areas with lower precipitation (883.5–1500 mm) were concentrated in the Pearl River Delta and plain regions (Fig. 5b). The average humidity ranged from 0.1 to 87.6%, with most regions experiencing high humidity levels (60–87.6%), while lower humidity areas (15–40%) were found in the central and eastern parts of the study area (Fig. 5c). The average wind speed ranged from 0.1 to 4.8 m/s, with the majority of areas experiencing moderate wind speeds (0.5–1.5 m/s). Low wind speed regions (0.1–0.5 m/s) were located in the north and east, and there were localized high wind speed areas (4–4.8 m/s) (Fig. 5d). Overall, the climate in the study area was characterized by high temperatures, ample precipitation, high humidity, and moderate wind speeds, though there were significant local variations.

From 2000 to 2020, the overall temperature change in the study area was not significant, with an average of approximately 22.1℃. However, there were fluctuations in specific years, with the highest temperature recorded at 23℃ in 2019 and the lowest at 21.35℃ in 2011 (Fig. 5e). Precipitation showed a significant linear change trend during this period, with an average value of 1830 mm. The highest precipitation was recorded in 2000 (3308.31 mm), and the lowest in 2006 (1068.52 mm) (Fig. 5f). Humidity showed a significant upward trend, with the annual average increasing from 72.06% to 77.48% (Fig. 5g). The annual average wind speed showed a significant downward trend, decreasing from 1.30 m/s to 1.05 m/s, with overall minor fluctuations (Fig. 5h). Overall, the changes in climate elements in the study area over the 21-year period exhibited certain regularities, but the trends and magnitudes of change varied among the different elements (Table 1).

Table 1 The standard of filtering weight coefficient assignment

QA	Pixel quality	Weight coefficient
0	better	1
1	ordinary	0.5
2–3	bad	0.2

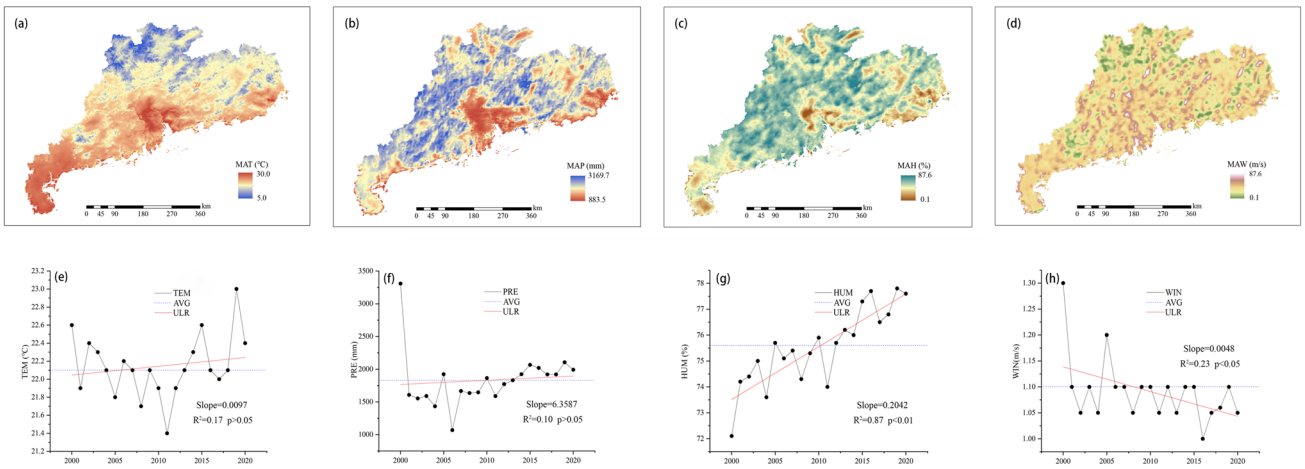
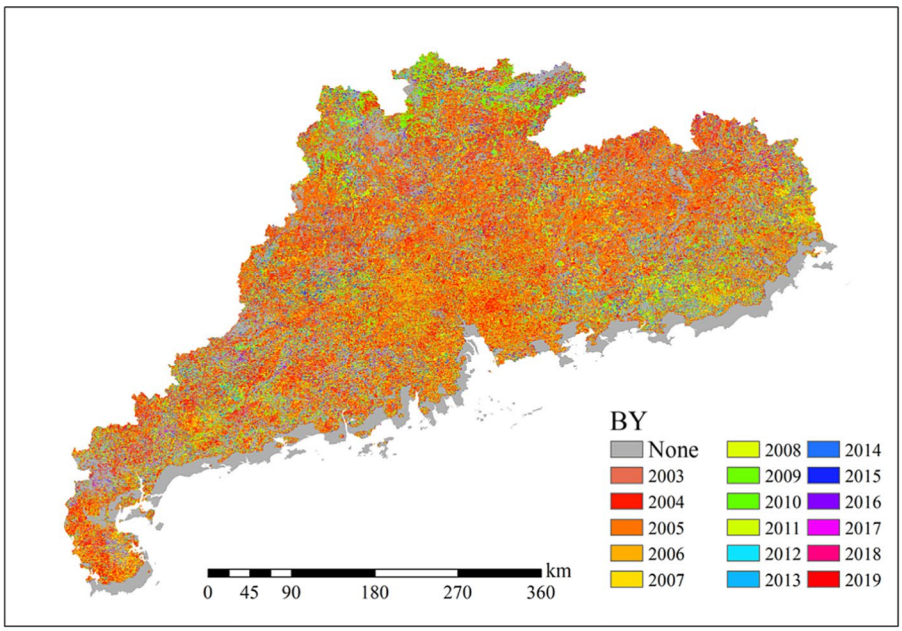


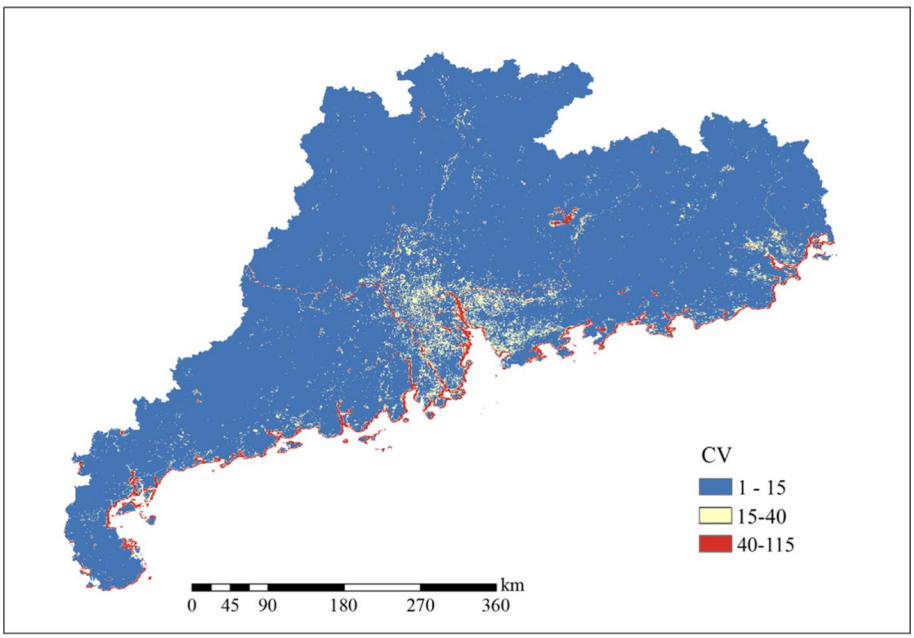
Fig. 5 Spatial distribution of average near surface temperature (a), average precipitation (b), average humidity (c) and average wind velocity (d) in Guangdong Province from 2000 to 2020. Trend of annual average near surface temperature(e), annual average precipitation (f), annual average precipitation (g) and annual average wind velocity (h) in Guangdong Province from 2000 to 2020

Break-points and variability of NDVI

Using the BFAST algorithm to analyze the NDVI change trends in the study area, the break-points of NDVI over the 21 years were calculated, and the results are shown in Fig. 6a. As shown in the figure, the NDVI break-point times in the study area between 2000 and 2020 mainly occurred between 2003 and 2019, with 22.87% of pixels having no break-points. Most of the break-points occurred in 2003, 2004, 2005, 2010, and 2019, accounting for 18.35%, 23.21%, 18.36%, 9.44%, and 8.57%, respectively, with the proportion of break-points in 2003, 2004, and 2005 all above 15%. Break-point pixels were evenly distributed throughout Guangdong Province, indicating that province-wide extreme



(a)



(b)

Fig. 6 Spatial distribution of NDVI break years in Guangdong Province from 2000 to 2020(a) Spatial distribution of NDVI coefficient of variation in Guangdong Province from 2000 to 2020(b)

climate changes and concentrated human economic activities strongly explained the vegetation changes in the study area.

The coefficient of variation of NDVI from 2000 to 2020 in the study area was calculated using the annual NDVI standard deviation and mean values, and the results are shown in Fig. 6b and Table 2. The coefficient of variation in the study area ranges from 1 to 115%, with the vast majority of pixel coefficients ranging from 1 to 15%, accounting for 78.39% of the pixels. This indicated that most of the vegetation growth in the study area was relatively stable, consistent with the conclusions of the spatiotemporal variation characteristics of the study area. Coefficient of variation between 15 and 40% indicated areas of unstable vegetation growth, mainly concentrated in the highly urbanized central Pearl River Delta region. In the analysis of spatiotemporal variation characteristics, the vegetation change rate in this region showed a declining trend, indicating that human factors are the main cause of unstable vegetation growth in the study area. Coefficient of variation between 40 and 115% indicated highly unstable vegetation growth areas, primarily located at the edges of rivers, lakes, and reservoirs, accounting for a smaller portion of pixels, at 7.55%.

Vegetation Changes in response to climatic factors in Guangdong Province

Vegetation changes in response to temperature in Guangdong Province

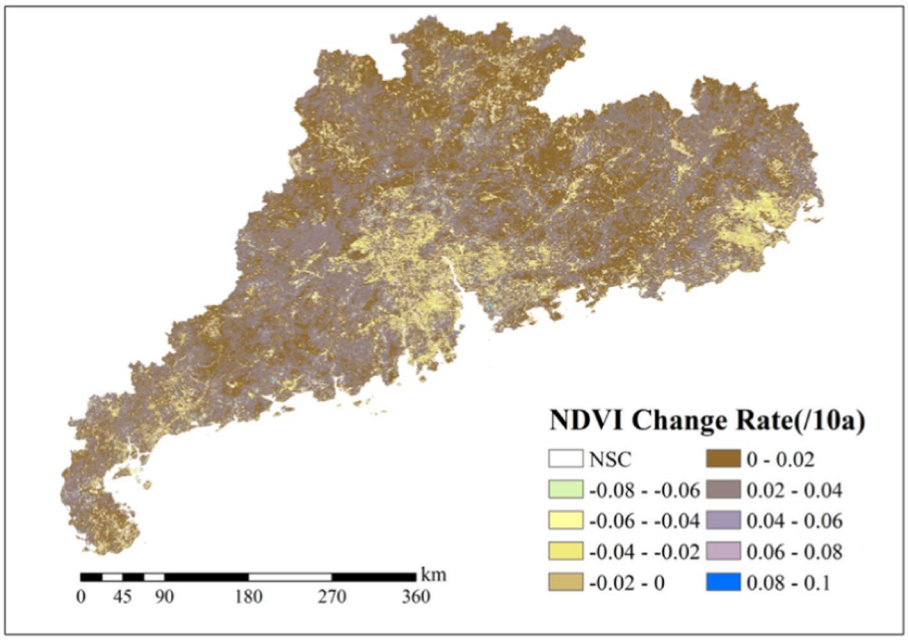
Using the RESTREND and TSS-RESTREND algorithms to analyze the impact of four climate factors on vegetation change in Guangdong Province, the effects of three climate factors, excluding temperature, on vegetation growth were stripped through residual analysis, and the obtained results were fitted using a univariate linear regression method, $p = 0.05$ was subjected to a significance test and both are added to obtain the response of interannual vegetation growth to temperature in Guangdong Province analyzed by CTSS-RESTREND. The results indicated that, on the annual scale, 83.3% of the pixels in the study area exhibited significant linear trends. Among these, 48.4% showed a significant upward trend, ranging from $0 \sim 0.1\ (10a)^{-1}$, with the majority of pixels having NDVI change rates distributed between $0 \sim 0.06(10a)^{-1}$; the proportion of pixels with a significant decrease in change rate is 34.9%, with a variation range of $-0.08 \sim 0(10a)^{-1}$, mainly between $-0.06 \sim 0.02\ (10a)^{-1}$ (Fig. 7a). they were mainly distributed in the Pearl River Delta region with high urbanization level in the central region and the boundary areas of the research area. On the growth seasonal scale, the proportion of significant pixels slightly increased during the growing season, reaching 84.2% The proportion of pixels with a significant increase in NDVI change rate also slightly increased, reaching 50.7% (Fig. 7b). The range of NDVI change rate for significantly increased pixels was consistent with the inter-annual NDVI change rate, and there was no significant difference in the main change range. However, there was a significant increase in the number of pixels within the range of $0.04 \sim 0.06\ (10a)^{-1}$ and $0.08 \sim 0.1(10a)^{-1}$, and the proportion of pixels in these two parts was 15.32% and 5.43% respectively. the spatial distribution of pixels showing a significant downward trend was also similar to vegetation changes driven by temperature throughout the year, but pixels with NDVI change rates between $-0.06 \sim -0.04\ (10a)^{-1}$ had a certain degree of improvement, accounting for 21.37% of these pixels, as shown in Table 3. During the growing season, vegetation response was more sensitive to temperature. Compared to year-round temperature driven vegetation changes, the positive and negative impacts on vegetation during the growing season had been improved to a certain extent, and the range of change rates increased was relatively high.

Table 2 Distribution range and pixel proportion of NDVI variability coefficient in the study area from 2000 to 2020

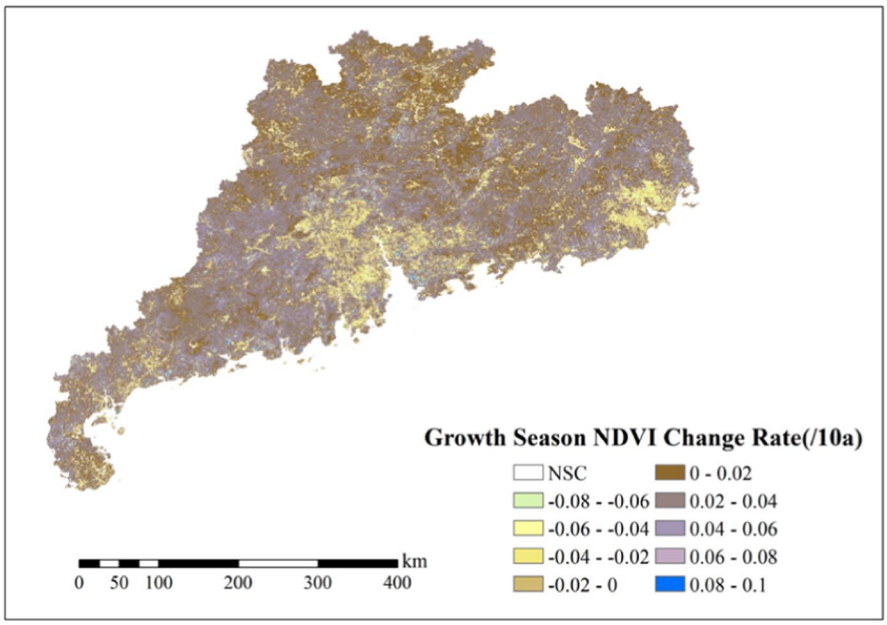
NDVI variability coefficient	Degree of stability	Proportion of Pixels
1–15%	stable	78.39%
15–40%	unstable	14.06%
40–115%	highly unstable	7.55%

Vegetation changes in response to precipitation in Guangdong Province

The vegetation change in response to precipitation in the study area was analyzed using the CTSS-RESTREND algorithm. The results reveal that, on the annual scale, the vegetation growth changes in the vast majority of the study area were affected by precipitation, with 84.6% of pixels showing a significant linear change trend. Among the pixels with a significant linear change trend, the pixels with a significant upward trend in NDVI change account for 63.9%, indicating that precipitation mainly had a positive impact on vegetation change in the study area. The NDVI change rate of these pixels was mainly in the range between $0 \sim 0.09\ (10a)^{-1}$, accounting for 53.01%; the amount of vegetation pixels affected by precipitation and showing a significant downward trend was relatively small. The pixel proportion was 20.7%, the variation range was $-0.08 \sim 0\ (10a)^{-1}$, mainly between $-0.08 \sim -0.04\ (10a)^{-1}$, and the pixel proportion was 16.21%, mainly distributed in the central and southern regions of the study area(Fig. 8a).



(a)



(b)

Fig. 7 The NDVI change rate in response to temperature in Guangdong Province from 2000 to 2020(a) Growth season NDVI change rate in response to temperature in Guangdong Province from 2000 to 2020(b)

The positive impact of precipitation on vegetation was much greater than the negative impact, and the change rate was relatively high, with some pixels having a change rate of over 0.12 $(10a)^{-1}$, indicating that precipitation was a major factor in promoting vegetation growth in the study area. on the growth seasonal scale, there was a slight increase in the proportion of significant pixels in vegetation changes during the growing season compared to the whole year, with an increase of 85.1% and an increase of 0.5%. Among them, the proportion of pixels with positive growth increased to 64.7%, while the proportion of pixels with significant decrease decreased to 20.4% (Fig. 8b). As shown in Table 4, among the pixels showing significant positive growth, there was a significant increase in the number of pixels distributed between 0.06–0.12 $(10a)^{-1}$ and > 0.12 $(10a)^{-1}$, accounting for 37.33% of the total

Table 3 Comparison of annual vegetation and growing season vegetation changes in response to temperature in Guangdong Province from 2000 to 2020

NDVI rate(/10a)	Annual vegetation change range Pixel proportion	Growth season change range Pixel proportion
−0.08–0.06	2.38%	2.92%
−0.06–0.04	19.36%	21.37%
−0.04–0.02	9.08%	7.21%
−0.02–0	4.08%	2%
0–0.02	13.85%	10.36%
0.02–0.04	21.42%	12.33%
0.04–0.06	5.12%	15.32%
0.06–0.08	5.31%	7.26%
0.08–0.1	2.70%	5.43%
NSC	16.70%	15.80%

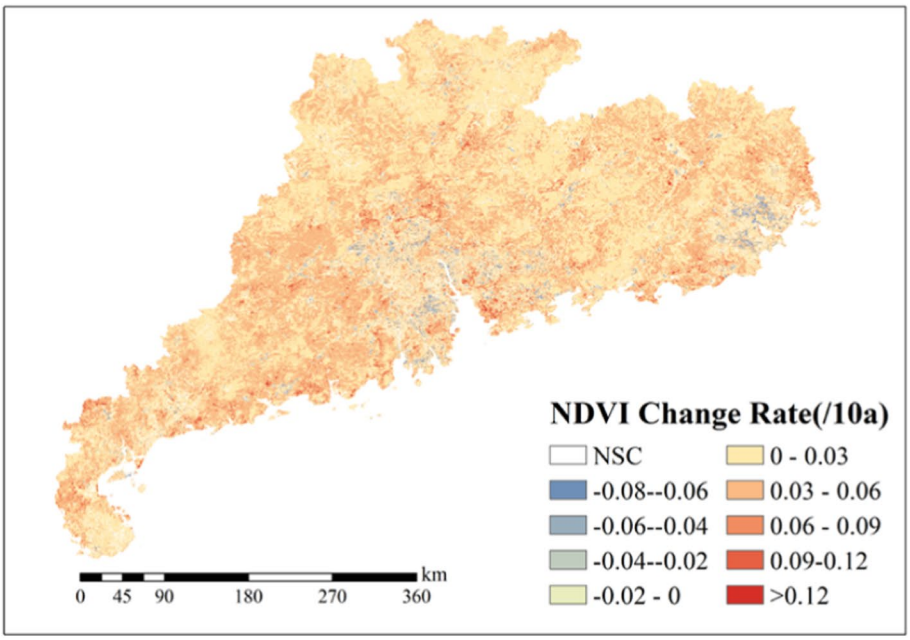
number of pixels; there was no significant difference in the overall spatial distribution and NDVI change rate distribution range of significantly reduced pixels compared to the annual vegetation change.

Vegetation changes in response to humidity in Guangdong Province

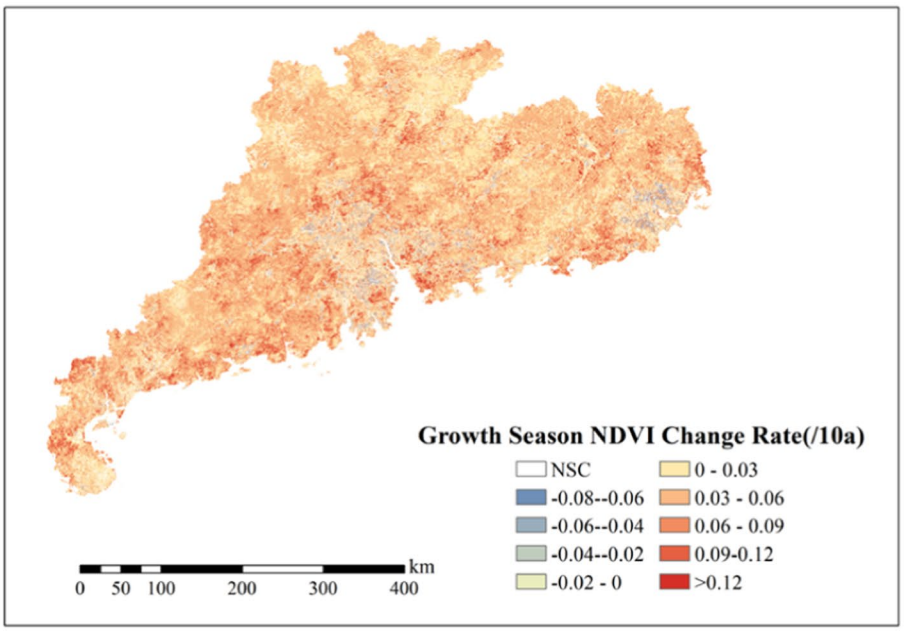
The vegetation change in response to humidity in the study area was analyzed using CTSS-RESTREND, and the results are shown in Fig. 9. The proportion of pixels with significant linear changes in vegetation affected by humidity was 84.9%, while the proportion of pixels with insignificant linear changes was 15.1%. Comparing Fig. 8a and Fig. 9a, it can be seen that the proportion of positive impact of humidity on vegetation in the study area was higher than that of precipitation, with a pixel proportion of 71.3%. However, the range of NDVI change rate affected by humidity was lower than that of precipitation, indicating that compared to humidity, precipitation had a greater impact on vegetation growth in the study area. In the range of NDVI change rate of pixels that showed positive growth due to humidity, the vast majority of pixels were mainly between 0 ~ 0.06 $(10a)^{-1}$, with a pixel proportion of 68.51%; The proportion of pixels showing a significant downward trend was 13.6%, and the range of NDVI change rate was between -0.08 ~ 0 $(10a)^{-1}$, mainly between -0.08 ~ -0.02 $(10a)^{-1}$. On the growth seasonal scale, the vegetation change in response to humidity during the growing season was mainly positive, with a pixel proportion of 71.8%, which was an increase of 0.5% compared to the annual change (Fig. 9b). The spatial distribution of NDVI change rate is not significantly different from the annual vegetation change, and the distribution range and number of pixels with a significant decrease are basically consistent with the interannual change rate. From Table 5, it can be seen that there is a certain difference in the change rate of significantly increased pixels compared to the annual vegetation change, mainly reflected in the increase in the number of pixels from 0.04 ~ 0.08 $(10a)^{-1}$, with the proportion of pixels in this part increasing to 29.35%. The driving force of humidity on vegetation growth was weaker compared to precipitation and temperature, and the distribution range of vegetation change rate is also lower.

Vegetation changes in response to wind speed in Guangdong Province

The inter-annual vegetation changes in response to wind speed in the study area was analyzed using CTSS-RESTREND. From the Fig. 10a, it can be seen that compared to the other three types of climate factors, wind speed mainly had a negative impact on the growth of vegetation in the study area, and the proportion of pixels with insignificant linear change trend was relatively high, accounting for 23.6%. Among the pixels with a significant linear change trend, the proportion of pixels with a significant increase trend was 31.2%, and the range of NDVI change rate was small, ranging between 0 ~ 0.02 $(10a)^{-1}$; the proportion of pixels showing a significant decreasing trend is 45.2%, with a range of variation between -0.06 ~ 0 $(10a)^{-1}$, mainly between -0.02 ~ 0 $(10a)^{-1}$, and the proportion of pixels is 35.48%. The impact of wind speed on vegetation was mainly negative, and the resulting vegetation change rate was relatively low, mostly between -0.02 ~ 0 $(10a)^{-1}$, indicating that wind speed was not the main factor causing vegetation change in the study area. On the growth seasonal scale, the number of pixels with significant linear changes in response to wind speed during the growing season in the study area had slightly increased, with the proportion of pixels increasing from 76.4% to 76.6%, and the significant pixels slightly increased by 0.2% (Fig. 10b). The distribution range of NDVI change rate is consistent with the distribution range of NDVI change rate throughout the year. From Table 6, it can be seen that the proportion of pixels with a significant decrease in vegetation change during the growing season had slightly increased to 45.4% compared to the annual vegetation change, with a slight increase in the proportion of pixels with a change rate range of -0.04 ~ 0 $(10a)^{-1}$. The proportion of pixel with change rate range 0.06 ~ 0.04 $(10a)^{-1}$ had slightly decreased. The proportion of rising pixels remained consistent with the annual vegetation change, both at 31.2%. Due to the small impact of wind speed on vegetation in the



(a)



(b)

Fig. 8 The NDVI change rate in response to precipitation in Guangdong Province from 2000 to 2020(a) Growth season NDVI change rate in response to precipitation in Guangdong Province from 2000 to 2020(b)

study area, vegetation changes during the growing season have not shown a more sensitive response to wind speed.

Discussion

Annual vegetation change trends in response to Climatic Factors

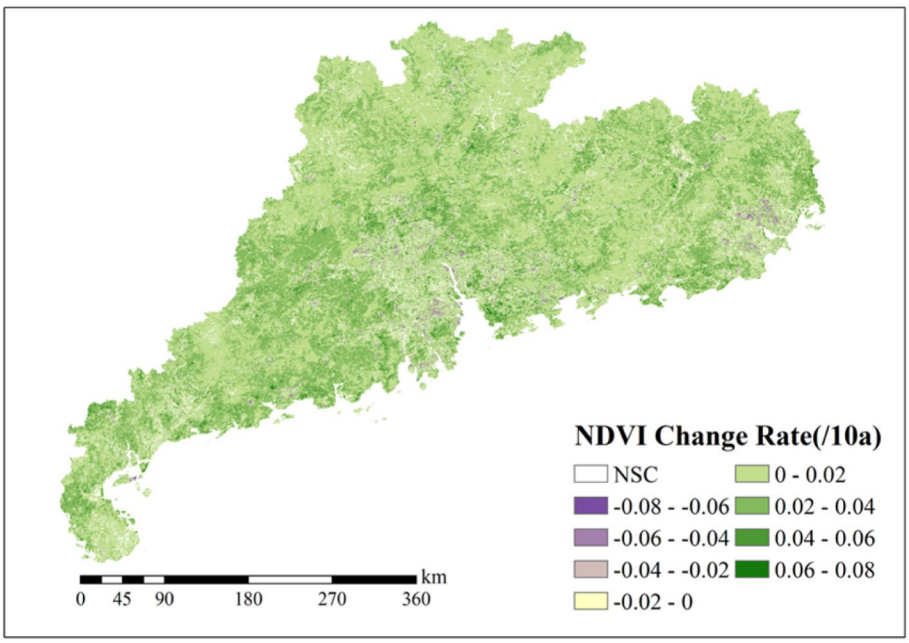
We found that temperature has both positive and negative effects on vegetation. The rate of change in vegetation

Table 4 Comparison of annual and growing season vegetation changes in response to precipitation in Guangdong Province from 2000 to 2020

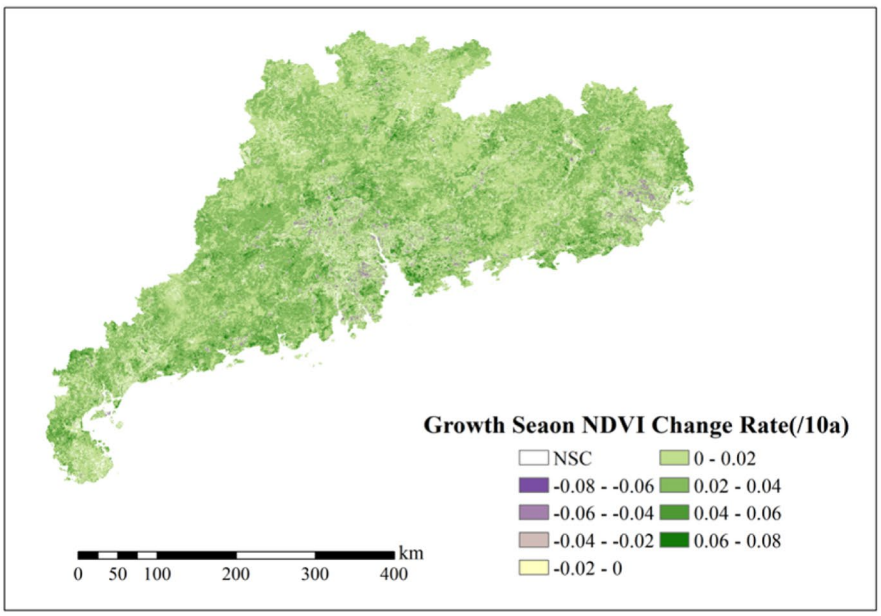
NDVI rate(/10a)	Annual vegetation change range Pixel proportion	Growth season change range Pixel proportion
−0.08 ~ −0.06	9.88%	8.29%
−0.06 ~ −0.04	6.33%	7.03%
−0.04 ~ −0.02	2.74%	3.11%
−0.02 ~ 0	1.75%	1.97%
0 ~ 0.03	27.39%	13.12%
0.03 ~ 0.06	16.34%	14.25%
0.06 ~ 0.09	9.28%	16.57%
0.09 ~ 0.12	6.36%	11.41%
> 0.12	4.53%	9.35%
NSC	15.40%	14.90%

growth driven by temperature in Guangdong Province ranges from -0.08 to 0.1 $(10a)^{-1}$, in which the proportion of pixels with a significant linear increase is 48.4%; the proportion of pixels with a significant decrease is 34.9%; and the proportion of pixels with no significant linear change is 16.7%. The proportion of pixels with a significant linear increase is close to that of pixels with a significant decrease, but the positive effect is slightly higher than the negative effect, indicating that the vegetation in the study area is mainly positively affected by temperature, with negative effects as a supplementary factor. Pixels with a significant decrease in the rate of change are mainly distributed in the highly urbanized Pearl River Delta region in the central part and the boundary areas of the study area. This may be due to the urban heat island effect caused by rising temperatures in urbanized areas (Gago et al. 2013). Extreme high temperatures may cause water stress in plants, leading to leaf dehydration and wilting, which in turn affects vegetation growth (Wang et al. 2015); the positive impact of precipitation on vegetation far outweighs the negative impact, with 63.9% of the pixels showing a significant increase; 20.7% of the pixels showing a significant decrease; and 15.4% of the pixels showing no significant change. Moreover, the rate of change in pixels with a significant increase is relatively high, with some pixels' change rates exceeding 0.12 $(10a)^{-1}$, indicating that precipitation is a major factor promoting vegetation growth in the study area. This is because adequate precipitation can boost soil moisture levels, enhancing the efficiency with which plants utilize water and fostering vegetation growth (Shi et al. 2024). Furthermore, precipitation aids in the dissolution and transportation of soil nutrients, thereby improving the nutrient absorption efficiency of plants (Medina-Roldán et al. 2024); humidity primarily has a positive impact on vegetation growth in the study area, with the proportion of significantly increasing pixels being higher than that of precipitation, accounting for 71.3%. However, the extent of vegetation change is noticeably lower than that of precipitation. This is because the mechanism by which humidity affects plant growth is relatively slow and indirect, mainly through altering soil moisture and plant transpiration. Precipitation, on the other hand, directly increases soil moisture, quickly enhancing plant water use efficiency and thus promoting vegetation growth (Nobel 1999). Additionally, the effect of increased humidity takes a longer time to manifest, while the impact of precipitation is more immediate and direct, resulting in a lower positive effect of humidity (Hulme et al. 1998); the impact of wind speed on vegetation growth in the study area is significantly less than that of the other three climatic factors, with 23.6% of pixels showing non-significant change. Among the pixels showing significant linear changes, the proportion of pixels with negative changes is higher than those with positive changes, accounting for 45.2%. Most of these pixels fall within the range of -0.02 ~ 0 $(10a)^{-1}$, accounting for 35.48%, indicating that wind speed mainly brings a low degree of negative impact on vegetation growth in the study area. The proportion of significantly increasing pixels is 31.2%, with a smaller distribution range between 0 ~ 0.02 $(10a)^{-1}$;the main negative impacts of wind speed on vegetation growth include mechanical damage, leaf reduction, and decreased photosynthesis efficiency. In coastal areas, strong winds can also cause salt damage. Additionally, high wind speeds can increase plant transpiration rates, leading to water stress and soil erosion, affecting plant growth (Gardiner et al. 2016). Nevertheless, the adverse effects of wind speed on vegetation growth are relatively minimal due to its indirect and gradual mechanisms, with mechanical damage and water loss requiring a longer period to become apparent. Vegetation can adapt to wind speed impacts by increasing leaf thickness and adjusting growth direction. In some areas, these effects may be offset by the positive impacts of other climatic factors (Vogel 2009).

Guangdong, located in southern China, belongs to the humid subtropical climate zone. This study found that in subtropical regions, precipitation and humidity play a positive role in vegetation growth, which aligns with the high dependency of vegetation on water conditions in subtropical regions (Hilker et al. 2016). The impact of temperature on vegetation varies by region, with its negative effects mainly concentrated in areas with higher levels of urbanization, likely due to the urban heat island effect. Our research findings differ from those of Xu et al. (2023), who investigated vegetation dynamics in Guizhou Province, a subtropical region similar to Guangdong. Through partial correlation analysis, they discovered that temperature exerts a greater positive impact on vegetation growth compared to precipitation, which showed limited



(a)



(b)

Fig. 9 The NDVI change rate in response to humidity in Guangdong Province from 2000 to 2020(a) Growth season NDVI change rate in response to humidity in Guangdong Province from 2000 to 2020(b)

or even negative effects. In contrast, our study employs the CTSS-RESTREND method, which more precisely isolates the independent influences of climate factors on vegetation, thereby minimizing the variable confounding that partial correlation analysis may neglect. The results of this study indicate that, similar to arid and semi-arid regions (Na et al. 2021), precipitation remains the primary driver of vegetation growth in subtropical regions. Given that Guangdong Province, located on the southern coastal region of China, frequently experiences typhoon disturbances, this study also incorporated wind speed as a climate factor. The results show that wind speed also negatively impacts vegetation growth in coastal areas, consistent with previous results (Zhang et al. 2022a, b).

Table 5 Comparison of annual vegetation and growing season vegetation changes in response to humidity in Guangdong Province from 2000 to 2020

NDVI rate(/10a)	Annual vegetation change range Pixel proportion	Growth season change range Pixel proportion
−0.08 ~ −0.06	5.36%	5.21%
−0.06 ~ −0.04	3.98%	3.87%
−0.04 ~ −0.02	2.95%	3.08%
−0.02 ~ 0	1.31%	1.44%
0 ~ 0.02	26.38%	24.34%
0.02 ~ 0.04	26.57%	18.11%
0.04 ~ 0.06	15.56%	24.61%
0.06 ~ 0.08	2.79%	4.74%
NSC	15.10%	14.60%

Vegetation change trends in response to climatic factors in growing season

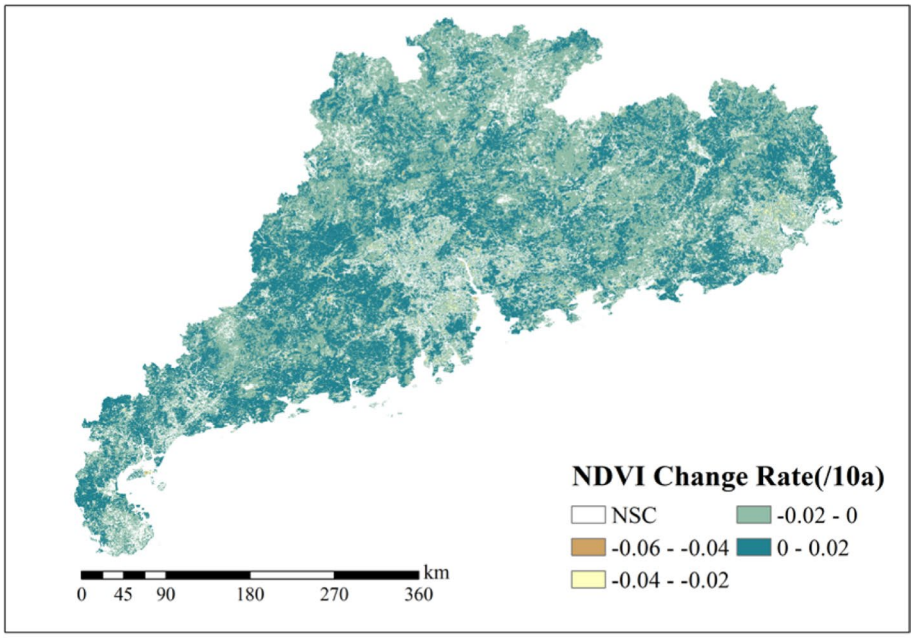
The vegetation changes during the growing season in response to the four climatic factors, compared to the annual changes, is mainly reflected in a slight increase in the proportion of significantly linear changing pixels and a minor variation in the overall range and pixel proportion. Compared to the impact of wind speed, the influence of temperature, precipitation, and humidity on vegetation changes during the growing season is more pronounced than that of the annual changes. This is because the growing season is a critical period for rapid plant growth and development, and climatic factors such as temperature, precipitation, and humidity have a more significant impact on vegetation during this period. At this time, the physiological activities of plants are the most active, and their response to external environmental changes is the most sensitive. Therefore, the impact of climatic changes on vegetation during the growing season is more evident (Wang et al. 2015).

The pixel count of the vegetation change rate in response to temperature ranging between 0.04 ~ 0.06 $(10a)^{-1}$ and 0.08 ~ 0.1 $(10a)^{-1}$ during the growing season has a noticeable increase compared to the annual data, with these two parts accounting for 7.26% and 5.43% respectively. During the growing season, elevated temperatures can accelerate photosynthesis and respiration, promoting rapid vegetation growth. Higher temperatures can also extend the growing season, giving plants more time to grow and develop. Therefore, the promoting effect of temperature on vegetation growth is more evident during the growing season, leading to an increase in the number of pixels within these change rate ranges compared to the annual data (Lambers. 2008); the pixel count of the vegetation change rate in response to precipitation ranging between 0.06 ~ 0.12 $(10a)^{-1}$ and > 0.12 $(10a)^{-1}$ has a significant increase compared to the annual data, with the proportion of pixels with increased change rates being 37.33%. During the growing season, increased precipitation can quickly replenish soil moisture, keeping the soil moist and promoting root growth and water absorption, especially during the periods when water demand is high. Adequate soil moisture can significantly promote vegetation growth (Shi et al. 2024). Additionally, in the growing season with high temperatures and high evaporation rates, sufficient precipitation can effectively alleviate plant water stress, improve water use efficiency, and thus promote vegetation growth (Lipiec et al. 2013); The pixel count of humidity-driven vegetation change rates ranging between 0.04 ~ 0.08 $(10a)^{-1}$ has a noticeable increase, with the proportion of pixels with increased change rates being 29.35%. The high humidity environment during the growing season can reduce plant transpiration, decrease water loss, and keep the leaves in a good water state, which is conducive to maintaining their normal physiological functions and rapid growth (Wu et al. 2015). Increased humidity can also enhance the opening of stomata on plant leaves, boosting photosynthesis efficiency, allowing carbon dioxide to enter the leaves more effectively for photosynthesis, thus promoting plant growth and biomass accumulation (Flexas and Carriqui 2020). In the hot and humid growing season, increased humidity can effectively alleviate plant water stress, improve water use efficiency, reduce water evaporation rates, and help plants maintain water balance better, thereby promoting vegetation growth (Nobel 1999).

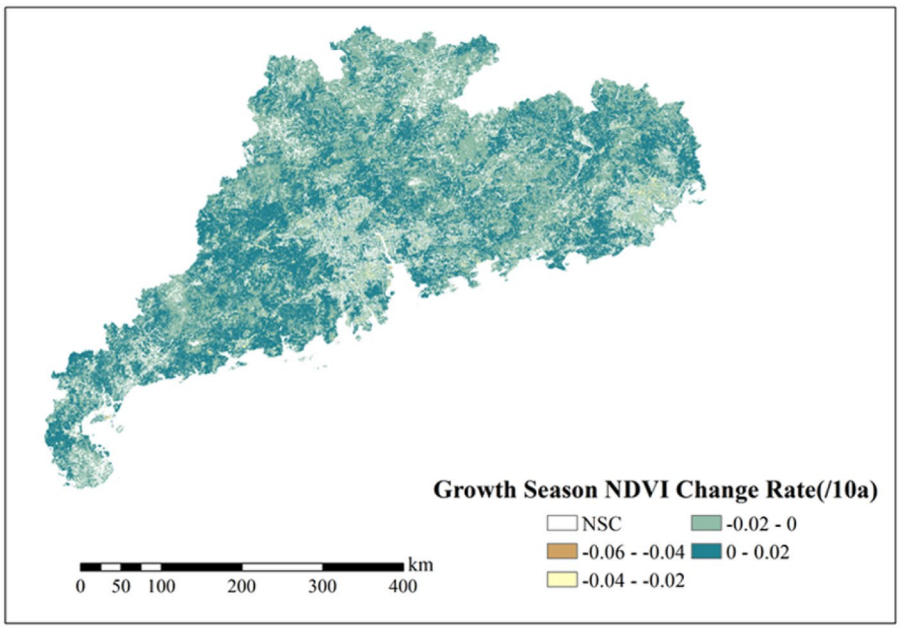
Limitations and uncertainties

The CTSS-RESTREND algorithm used in this study is limited by the virtual variable settings of the TSS-RESTREND algorithm and the computational principles of the BFAST algorithm. When the time series is relatively short, the number of break-points calculated by the BFAST algorithm is significantly reduced, making it impossible to segment the time series residuals. This causes the CTSS-RESTREND algorithm to fail to function properly. Therefore, this study did not analyze the seasonal vegetation changes in response to climatic factors. Future related research could focus on optimizing the BFAST algorithm or proposing other time series segmentation methods to make the CTSS-RESTREND algorithm suitable for short time series analysis.

This study is constrained by data availability and did not consider the effects of other factors such as land use, slope, and other aspects on climate-driven vegetation changes. Additionally, due to the lack of detailed human activity data, the impact of human activities on vegetation changes



(a)



(b)

Fig. 10 NDVI change rate in response to wind speed in Guangdong Province from 2000 to 2020(a) Growth season NDVI change rate in response to wind speed in Guangdong Province from 2000 to 2020(b)

was not analyzed. It is noteworthy that human activities do not only directly influence vegetation distribution through changes in land use patterns but also indirectly affect vegetation dynamics by influencing climate factors such as the urban heat island effect and warming effects from greenhouse gas emissions. Furthermore, the accuracy and reliability of results can be improved by validating remote sensing findings with ground-based ecological data. Such validation could involve field studies in key areas to confirm vegetation trends or collaboration with local ecological research stations to integrate ground measurements. Future related research could extend and

Table 6 Comparison of interannual vegetation and growing season vegetation changes in responses to wind velocity in Guangdong Province from 2000 to 2020

NDVI rate(/10a)	Annual vegetation change range Pixel proportion	Growth season change range Pixel proportion
−0.06 ~ -0.04	3.37%	3.16%
−0.04 ~ -0.02	6.35%	6.41%
−0.02 ~ 0	35.48%	35.83%
0 ~ 0.02	31.20%	31.20%
NSC	23.60%	23.40%

optimize these aspects to gain a better understanding of the driving mechanisms behind vegetation changes.

Conclusion

This study primarily used the CTSS-RESTREND algorithm to detect the impact of four climate factors on vegetation changes in Guangdong Province from 2000 to 2020. Unlike traditional correlation analysis methods, the CTSS-RESTREND algorithm effectively isolates the impact of individual climate factors by eliminating the residual effects of other variables, residual effects of other variables denote the influence of the three non-target climate factors, as well as additional factors such as human activities, on NDVI variations. The study results indicate that precipitation is the most significant positive driving factor, positively impacting 63.9% of the pixels. Humidity also positively impacted 71.3% of the pixels, although its influence was slower and less significant compared to precipitation. The impact of temperature is mixed, significantly negatively affecting 34.9% of the pixels, especially in the Pearl River Delta region, but also positively affecting 48.4% of the pixels. Wind speed mainly had a negative impact, affecting 45.2% of the pixels negatively, but the degree of impact was relatively slight. On the growing season, vegetation becomes more sensitive to temperature, precipitation, and humidity due to the active plant growth and heightened physiological activity occurred in this period. However, the influence of wind speed on vegetation does not show significant enhancement.

The results of this study contribute to a more comprehensive understanding of the mechanisms through which vegetation ecology in Guangdong Province responds to climate change, with particular emphasis on the dominant role of precipitation. This understanding provides a scientific foundation for arrangements of agricultural planting and the development of ecological protection policies and management strategies. Changes in precipitation patterns may lead to significant shifts in vegetation, and the negative impacts of temperature on urban vegetation, particularly the inhibitory effects of high temperatures on plant growth and biodiversity, must also be considered. Accordingly, policies in Guangdong Province should prioritize enhancing ecosystem resilience, with particular focus on water resource management, ecosystem service valuation, and biodiversity conservation. The CTSS-RESTREND method employed in this study is equally applicable to other regions, enabling the exploration of the independent impacts of various climate factors on vegetation dynamics. Additionally, the results regarding the dominant role of precipitation and the mixed effects of temperature can serve as a valuable reference for other subtropical regions, where similar climate-vegetation interactions may occur.

Acknowledgements We acknowledge R for offering free and open-source software.

Author contributions Conceptualization, B.H. and Y.K; Methodology, B.H. and S.D.; Software, B.H., S.D. and Z.R.; Validation, B.H., S.D. and Y.K.; Formal Analysis, B.H, and S.D.; Investigation, B.H., Z.W and Z.R.; Resources, B.H., S.D. and Z.W.; Data Curation S.D. and Z.W.; Writing – Original Draft Preparation, B.H.; Writing – Review & Editing, B.H., S.D., Z.W. and Y.K.; Visualization, B.H., S.D. and Z.R.; Supervision, Y.K. and L.M.; Project Administration, Y.K.; Funding Acquisition, L.M.

Funding This research was funded by the National Natural Science Foundation of China (No. 21936004) and the Fundamental Research Funds for the Central Universities (No. 21623118).

Data availability NDVI data used in this study were obtained from the MOD13Q1 product provided by NASA LP DAAC (https://doi.org/https://doi.org/10.5067/MODIS/MOD13Q1.061) and accessed via Google Earth Engine (https://earthengine.google.com). Climate factor data used in this study can be freely obtained from National Earth System Science Data Center(https://www.geodata.cn).

Declarations

Conflicts of Interest The authors declare no conflict of interest.

Ethical approval There is no ethical violation in our study.

Open Access This article is licensed under a Creative Commons Attribution 4.0 International License, which permits use, sharing, adaptation, distribution and reproduction in any medium or format, as long as you give appropriate credit to the original author(s) and the source, provide a link to the Creative Commons licence, and indicate if changes were made. The images or other third party material in this article are included in the article's Creative Commons licence, unless indicated otherwise in a credit line to the material. If material is not included in the article's Creative Commons licence and your intended use is not permitted by statutory regulation or exceeds the permitted use, you will need to obtain permission directly from the copyright holder. To view a copy of this licence, visit http://creativecommons.org/licenses/by/4.0/.

References

Abeli T, Mondoni A, Rossi G et al (2014) Effects of summer heat waves on Europe's wild flora and vegetation. Agrochimica 58:128–132

Boulion VV (2017) Effect of geographical factors on the biological productivity of Lake ecosystems: Modeling and forecast. Contemp Probl Ecol 10(2):111–118

Burrell AL, Evans JP, Liu Y (2017) Detecting dryland degradation using Time Series Segmentation and Residual Trend analysis (TSS-RESTREND). Remote Sens Environ 197:43–57

Cao XM, Chen X, Bao AM et al (2011) Response of vegetation to temperature and precipitation in Xinjiang during the period of 1998–2009. J Arid Land 3(2):94–103

Chapin FS, Starfield AM (1997) Time lags and novel ecosystems in response to transient climatic change in Arctic Alaska. Clim Change 35(4):449–461

Chen H, Liu XN, Ding C et al (2018) Phenology-Based Residual Trend Analysis of MODIS-NDVI Time Series for Assessing Human-Induced Land Degradation. Sensors 18(11):3676

Chu H, Venevsky S, Wu C et al (2019) NDVI-based vegetation dynamics and its response to climate changes at Amur-Heilongjiang River Basin from 1982 to 2015. Sci Total Environ 650:2051–2062

Chuai XW, Huang XJ, Wang WJ et al (2013) NDVI, temperature and precipitation changes and their relationships with different vegetation types during 1998–2007 in Inner Mongolia. China International Journal of Climatology 33(7):1696–1706

Davis MB (1989) Lags in vegetation response to greenhouse warming. Clim Change 15(1):75–82

De Jong R, Schaepman ME, Furrer R et al (2013) Spatial relationship between climatologies and changes in global vegetation activity. Glob Change Biol 19(6):1953–1964

Duan H, Xue X, Wang T et al (2021) Spatial and temporal differences in alpine meadow, alpine steppe and all vegetation of the qinghai-tibetan plateau and their responses to climate change. Remote Sensing 13(4):669

Flexas J, Carriqui M (2020) Photosynthesis and photosynthetic efficiencies along the terrestrial plant's phylogeny: lessons for improving crop photosynthesis. Plant J 101(4):964–978

Gago EJ, Roldan J, Pacheco-Torres R et al (2013) The city and urban heat islands: A review of strategies to mitigate adverse effects. Renew Sustain Energy Rev 25:749–758

Gao X, Huang X, Lo K et al (2021) Vegetation responses to climate change in the Qilian Mountain Nature Reserve. Northwest China Global Ecology and Conservation 28:e01698

Gardiner B, Berry P, Moulia B (2016) Review: Wind impacts on plant growth, mechanics and damage. Plant Sci 245:94–118

Gong X, Li Y, Wang X et al (2022) Quantitative assessment of the contributions of climate change and human activities on vegetation degradation and restoration in typical ecologically fragile areas of China. Ecol Ind 144:109536

Guan Y, Lu H, Yin C et al (2020) Vegetation response to climate zone dynamics and its impacts on surface soil water content and albedo in China. Sci Total Environ 747:141537

Guo JT, Wang KB, Wang TJ et al (2022) Spatiotemporal Variation of Vegetation NDVI and Its Climatic Driving Forces in Global Land Surface. Pol J Environ Stud 31(4):3541–3549

Han FF, Yan JJ, Ling HB et al (2021) Variance of vegetation coverage and its sensitivity to climatic factors in the Irtysh River basin. PeerJ 9:e11334

Hans Lambers F, Chapin S, Pons TL (2008) Plant Physiological Ecology. Springer New York, New York, NY. https://doi.org/10.1007/978-0-387-78341-3

He D, Yi G, Zhang T et al (2018) Temporal and spatial characteristics of evi and its response to climatic factors in recent 16 years based on grey relational analysis in inner mongolia autonomous region. China Rem Sens 10(6):961

Hilker T, Lyapustin AI, Tucker CJ et al (2014) Vegetation dynamics and rainfall sensitivity of the Amazon. Proc Natl Acad Sci USA 111(45):16041–16046

Hou MT, Zhao HY, Wang Z et al (2013) Vegetation responses to climate change by using the satellite-derived normalized difference vegetation index: a review. Clim Environ Res 18(3):353–364

Huang J, Shi TL, Gong B et al (2018) Fitting an Optical Fiber Background with a Weighted Savitzky-Golay Smoothing Filter for Raman Spectroscopy. Appl Spectrosc 72(11):1632–1644

Hulme M, Osborn TJ, Johns TC (1998) Precipitation sensitivity to global warming: Comparison of observations with HadCM2 simulations. Geophys Res Lett 25(17):3379–3382

Ibrahim YZ, Balzter H, Kaduk J et al (2015) Land degradation assessment using residual trend analysis of GIMMS NDVI3g, soil moisture and rainfall in sub-Saharan west Africa from 1982 to 2012. Remote Sensing 7(5):5471–5494

Ichii K, Kawabata A, Yamaguchi Y (2002) Global correlation analysis for NDVI and climatic variables and NDVI trends: 1982–1990. Int J Remote Sens 23(18):3873–3878

Ivits E, Cherlet M, Horion S et al (2014) Global biogeographical pattern of ecosystem functional types derived from earth observation data. Remote Sens 5(7):3305–3330

Kong DX, Miao CY, Wu JW et al (2020) Time lag of vegetation growth on the Loess Plateau in response to climate factors: estimation, distribution, and influence. Sci Total Environ 2020(744):140726

Kundu A, Patel NR, Saha SK et al (2017) Desertification in western Rajasthan (India): an assessment using remote sensing derived rain-use efficiency and residual trend methods. Nat Hazards 86(1):297–313

Kuzyakov Y, Gavrichkova O (2010) Time lag between photosynthesis and carbon dioxide efflux from soil: a review of mechanisms and controls. Glob Change Biol 16(12):3386–3406

Li C, Kuang YQ, Huang NS et al (2013) The long-term relationship between population growth and vegetation cover: an empirical analysis based on the panel data of 21 Cities in Guangdong Province, China. Int J Environ Res Public Health 10(2):660–677

Li XB, Li RH, Li GQ et al (2016) Human-induced vegetation degradation and response of soil nitrogen storage in typical steppes in Inner Mongolia, China. J Arid Environ 124:80–90

Li L, Chan PW, Deng T et al (2021) Review of advances in urban climate study in the guangdong-hong kong-macau greater bay area. China Atmospheric Res 261:105759

Lipiec J, Doussan C, Nosalewicz A, Kondracka K (2013) Effect of drought and heat stresses on plant growth and yield: a review. International Agrophysics 27(4):463

Liu TB, Han ZL, Peng F et al (2017) The composition and important research issues of human-ocean regional system. Scientia Geographica Sinica 37(10):1527–1534

Liu CX, Melack J, Tian Y et al (2019) Detecting land degradation in eastern china grasslands with time series segmentation and residual trend analysis (TSS-RESTREND) and GIMMS NDVI3g data. Remote Sensing 11(9):1014

Londhe DS, Katpatal YB, Mukesh MS, Bokde ND (2024) Vegetation dynamics and its driving factors in agro-climatic zones of Upper Bhima Sub-basin, Western India. Int J Environ Sci Technol 21(3):2367–2382

Ma WY, Wang XM, Zhou N et al (2017) Relative importance of climate factors and human activities in impacting vegetation dynamics during 2000–2015 in the Otindag Sandy Land, northern China. J Arid Land 9(4):558–567

Mao F, Lu ZG, Zhang JH et al (2007) Relations between AVHRR NDVI and climate factors in Northern Tibet in recent 20 years. Acta Ecol Sin 27(8):3198–3205

Martinez AD, Labib SM (2023) Demystifying normalized difference vegetation index (NDVI) for greenness exposure assessments and policy interventions in urban greening. Environ Res 220:115155

Medina-Roldán E, Wang M, Miyasaka T, Pan Y, Li X, Liu B, Qu H (2024) Precipitation controls topsoil nutrient buildup in arid and semiarid ecosystems. Agriculture 14(12):2364

Meng B, Ge J, Liang T et al (2017) Evaluation of remote sensing inversion error for the above-ground biomass of alpine meadow grassland based on multi-source satellite data. Remote Sensing 9(4):372

Mohammat A, Wang X, Xu X et al (2013) Drought and spring cooling induced recent decrease in vegetation growth in inner Asia. Agric for Meteorol 178:21–30

Morovati M, Karami P (2024) Trend analysis of temperature and vegetation cover in the distribution range of Apis florea in Iran. Int J Environ Sci Technol 21(9):6745–6758

Na R, Na L, Du H, He HS, Shan Y, Zong S, Huang L, Yang Y, Wu Z (2021) Vegetation greenness variations and response to climate change in the arid and semi-arid transition zone of the mongo-lian plateau during 1982–2015. Remote Sensing 13(20):4066

Nobel P S. (1999). Physicochemical and Environmental Plant Physiology. Academic Press, pp 44–99

Piao S, Wang X, Park T et al (2020) Characteristics, drivers and feedbacks of global greening. Nature Revi Environ 1(1):14–27

Ruan Z, Kuang YQ, He YY et al (2020) Detecting Vegetation Change in the Pearl River Delta Region Based on Time Series Segmentation and Residual Trend Analysis (TSS-RESTREND) and MODIS NDVI. Remote Sensing 12(24):4049

Sedighifar Z, Motlagh MG, Halimi M (2020) Investigating spatiotemporal relationship between EVI of the MODIS and climate variables in northern Iran. Int J Environ Sci Technol 17(2):733–744

Shi Z, Liang G, Li S, Liu W (2024) Adequate water supply enhances seedling growth and metabolism in Festuca kryloviana: insights from physiological and transcriptomic analys. BMC Plant Biol 24(1):714

Song Y, Ma M (2011) A statistical analysis of the relationship between climatic factors and the Normalized Difference Vegetation Index in China. Int J Remote Sens 32(14):3947–3965

Sun W, Song X, Mu X et al (2015) Spatiotemporal vegetation cover variations associated with climate change and ecological restoration in the Loess Plateau. Agric for Meteorol 209:87–99

Sun GQ, Li L, Li J et al (2022) Impacts of climate change on vegetation pattern: Mathematical modeling and data analysis. Phys Life Rev 43:239–270

Sun L, Li H, Wang J et al (2023) Impacts of climate change and human activities on NDVI in the Qinghai-Tibet Plateau. Remote Sensing 15(3):587

Tang H, Li Z, Zhu Z et al (2015) Variability and climate change trend in vegetation phenology of recent decades in the Greater Khingan Mountain area. Northeastern China Remote Sens 7(9):11914–11932

Tietjen B, Schlaepfer D, Bradford J et al (2017) Climate change-induced vegetation shifts lead to more ecological droughts despite projected rainfall increases in many global temperate drylands. Glob Change Biol 23(7):2743–2754

Verbesselt J, Hyndman R, Newnham G et al (2010) Detecting trend and seasonal changes in satellite image time series. Remote Sens Environ 114(1):106–115

Vogel S (2009) Leaves in the lowest and highest winds: temperature, force and shape. New Phytol 183(1):13–26

Wang J, Wang K, Zhang M et al (2015) Impacts of climate change and human activities on vegetation cover in hilly southern China. Ecol Eng 81:451–461

Wen Z, Wu S, Chen J et al (2017) NDVI indicated long-term interannual changes in vegetation activities and their responses to climatic and anthropogenic factors in the Three Gorges Reservoir Region, China. Sci Total Environ 574:947–959

Wu DH, Zhao X, Liang SL et al (2015) Time-lag effects of global vegetation responses to climate change. Glob Change Biol 21(9):3520–3531

Xu X, Liu H, Lin Z et al (2019) Relationship of abrupt vegetation change to climate change and ecological engineering with multi-timescale analysis in the karst region. Southw China Remote Sens 11(13):1564

Xue X, Wang Z, Hou S (2023) NDVI-based vegetation dynamics and response to climate changes and human activities in Guizhou Province. China Forests 14(4):753

Yan Y, Liu H, Bai X et al (2023) Exploring and attributing change to fractional vegetation coverage in the middle and lower reaches of Hanjiang River Basin. China Environ Monitor Assessm 195(1):131

Yang K, Guan DS (2006) Biomass distribution and its functioning of forest understory vegetation. Chin J Ecol 25(10):1252–1256

Zhang Y, Ye A (2020) Spatial and temporal variations in vegetation coverage observed using AVHRR GIMMS and Terra MODIS data in the mainland of China. Int J Remote Sens 41(11):4238–4268

Zhang Q, Zhang W, Chen YD et al (2011) Flood, drought and typhoon disasters during the last half-century in the Guangdong province. China. Natural Hazards 57(2):267–278

Zhang LF, Yan HW, Qiu LS et al (2022a) Spatial and temporal analyses of vegetation changes at multiple time scales in the qilian mountains. Remote Sensing 13(24):5046

Zhang T, Xu X, Jiang HL et al (2022b) Widespread decline in winds promoted the growth of vegetation. Sci Total Environ 825:153682

Zhang D, Zhao Y, Qi H, Shan L, Chen G, Ning T (2024) Effects of Micro-Topography and Vegetation on Soil Moisture on Fixed Sand Dunes in Tengger Desert. China Plants 13(11):1571

Zhao J, Liu D, Zhu Y, Peng H, Xie H (2022) A review of forest carbon cycle models on spatiotemporal scales. J Clean Prod 339:130692

Zhong L, Ma Y, Salama MS et al (2010) Assessment of vegetation dynamics and their response to variations in precipitation and temperature in the Tibetan Plateau. Clim Change 103(3–4):519–535

Publisher's Note Springer Nature remains neutral with regard to jurisdictional claims in published maps and institutional affiliations.